

Effect of calcination temperature on the catalytic performance of CoFe₂O₄/Nitrogen doped sludge based activated carbon in activation of peroxymonosulfate for degradation of coking wastewater

Yongkang Tao¹, Lihua Li^{1,a}, Lixiong Ren¹, Yu Liang¹ and Xin Wang¹

1. School of Chemical Engineering, University of Science and Technology Liaoning, Anshan Liaoning 114051, China

Abstract. A novel supported heterogeneous magnetic catalyst CoFe₂O₄/N-doped sludge based activated carbon (CoFe₂O₄/N-SAC) was prepared by polymer network gel method for the first time. The physicochemical properties of the materials were characterized by means of XRD, SEM, TEM, VSM and XPS techniques. The prepared catalyst is applied to the heterogeneous activation of peroxymonosulfate for degradation of coking wastewater, and the effect of calcination temperature on the catalytic activity was investigated. The result reveals that the catalyst shows the highest catalytic activities under the calcination temperature is 800 °C with the TOC removal rate of coking wastewater is 84.31%.

1. Introduction

Over the past period of time, the advanced oxidation processes (AOPs) based on peroxymonosulfate (PMS) have been widely concerned for degradation of coking wastewater because the sulfate radical (SO₄^{-•}) is an oxidizing agent with a high ability to oxidize organic pollutants due to its higher oxidation-reduction potential and longer half-life period (the oxidation-reduction potential and half-life period of SO₄^{-•} are 2.6-3.1eV and 4s, respectively), and its use avoids some shortcomings of traditional Fenton and ozone, which both use hydroxyl radicals (•OH) to degrade organic pollutants with the half-life of •OH is short and the redox potential is low (the half-life and redox potential of •OH were 1μs and 1.8~2.7 eV, respectively) [1-2]. Transition metal ions combined with persulfate to form SO₄^{-•} is a highly efficient method for the degradation of organic pollutants and Co²⁺ is the best catalyst for activating persulfate [3]. However, the detrimental impact of Co²⁺ lost with the effluent on environment and human health is a serious concern. Thus it is essential to develop heterogeneous Co catalysts [1].

heterogeneous Co-base catalysts such as Co₃O₄, CoFe₂O₄ coupled with PMS have been investigated [4-5] and the spinel-structured nano-ferrite CoFe₂O₄ has been widely used in wastewater treatment because of its excellent catalytic performance [6]. Activated carbon has been used as a carrier for heterogeneous catalysts because of its huge specific surface area [7-12]. In addition, the research has been shown that doping heteroatoms such as N into the carbon network can create more active sites and bring new properties such as higher selectivity towards reduction reaction [13-14]. Sludge contains a large amount of organic matter, which can be used as raw material for the preparation of sludge based activated carbon (SAC) [15]. Supporting CoFe₂O₄ on SAC can not only solves the problems of easy agglomeration and poor stability of unsupported CoFe₂O₄, but also solves the conundrum of SAC separation, which is beneficial to the practical application of the catalyst.

In this study, the CoFe₂O₄/N-SAC was prepared and used to activate PMS to generate SO₄^{-•} for degradation of coking wastewater. The effect of calcination temperature was investigated.

Effluent treatment applications of multifarious

^a Corresponding author: lilh2011@163.com

2. Methods

2.1 Materials

Sewage sludge used in this study is collected from coking plant of Anshan iron and Steel Group (Anshan, China). Coking wastewater is taken from the aerobic tank effluent of Anshan Iron and Steel coking plant (Anshan, China). $\text{HKSO}_5 \cdot 0.5\text{K}_2\text{SO}_4 \cdot 0.5\text{HKSO}_4$ was purchased from Sigma-Aldrich, $\text{Co}(\text{NO}_3)_2 \cdot 6\text{H}_2\text{O}$, $\text{Fe}(\text{NO}_3)_3 \cdot 9\text{H}_2\text{O}$, Citric acid, acrylamide and ammonium persulfate were analytical grade and purchased from rchased from Sinopharm Chemical Reagent Co., Ltd. (Shanghai, China), and DI water was used throughout.

2.2 Preparation of catalysts

Sewage sludge of biological wastewater treatment plant and agricultural waste were used as the raw material to product SAC via chemical activated process with ZnCl_2 as activation agent within a muffle furnace under $600\text{ }^\circ\text{C}$ for 1.5 h with the protection of N_2 before cooled to room temperature.

$\text{CoFe}_2\text{O}_4/\text{N-SAC}$ was prepared by Polymer network gel method using $\text{Co}(\text{NO}_3)_2 \cdot 6\text{H}_2\text{O}$ and $\text{Fe}(\text{NO}_3)_3 \cdot 9\text{H}_2\text{O}$ as the precursors and Citric acid as the complexant. The appropriate amounts of $\text{Co}(\text{NO}_3)_2 \cdot 6\text{H}_2\text{O}$, $\text{Fe}(\text{NO}_3)_3 \cdot 9\text{H}_2\text{O}$ and citric acid (Co: Fe: citric acid=1:2:3, by mole) were dissolved in 100 mL distilled water under vigorous stirring in a $80\text{ }^\circ\text{C}$ water bath with the concentrations of precursor solution is 15%, the ammonia was used to regulate pH at 7, 10 g SAC was immersed in the solution and then 7.5 g acrylamide and 0.075 g ammonium persulfate was added to the system. After a few minutes, the uniform wet gel formed by polymerization was dried at $80\text{ }^\circ\text{C}$ for 12h. Finally, it was transferred to muffle furnace and calcined at $600\text{-}900\text{ }^\circ\text{C}$ for 2 h with the absence of oxygen condition to obtain the catalysts.

2.3 Degradation experiment of coking wastewater

The oxidation of coking wastewater was carried out in conical bottles. The catalyst and oxidant were added into the coking wastewater. The reaction was conducted in the $25\text{ }^\circ\text{C}$ constant temperature water bath oscillator. 50 mL

suspension samples were taken out at specific time intervals and quenched with 1 mL of ethanol to prevent further reaction. The TOC was determined with a total organic carbon analyzer (Sievers InnovOx, GE, America).

2.4 Characterization of catalyst

The crystal structure of catalysts was analyzed by a powder X-ray diffractometer (XRD, RigakuD/max-2000) with monochromatic Cu K α radiation (45 kV, 50 mA). The morphology of the catalysts was characterized by a Jeol 2100 TEM with field emission gun at 200 kV. The surface morphology of the catalysts was investigated using a scanning electron microscopy (SEM, Evo 18, Gemarny). The room temperature magnetic properties of the samples were investigated using vibrating sample magnetometry (VSM, 730T, America) at magnetic fields up to 15kOe. The elemental compositions of $\text{CoFe}_2\text{O}_4/\text{N-SAC}$ were detected by XPS on a Thermo Escalab 250.

3. Results and discussions

3.1 Characterization of SAC and $\text{CoFe}_2\text{O}_4/\text{N-SAC}$

3.1.1 XRD

Figure 1 shows the XRD patterns of $\text{CoFe}_2\text{O}_4/\text{N-SAC}$ with various calcination temperatures, all the catalysts exhibited the typical patterns of cubic phase of CoFe_2O_4 with spinel structure and the space group Fm3m (JCPDS No.00-003-0864).

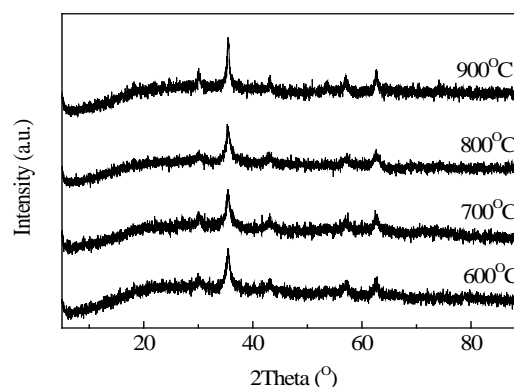


Figure 1. XRD patterns of $\text{CoFe}_2\text{O}_4/\text{N-SAC}$ calcined at different temperatures

It can be seen from the diagram that with the increase of temperature, the diffraction peaks of $\text{CoFe}_2\text{O}_4/\text{N-SAC}$ became more narrow and intense, indicating that the particle size of CoFe_2O_4 becomes bigger. When the temperature is further increased from 800 to 900 °C, the diffraction peak intensity of each crystal plane increased remarkably, which caused by the agglomeration of CoFe_2O_4 on the surface of catalyst [16].

3.1.2 XPS

In order to investigate chemical states and the compositions in the content on the surface of the SAC and $\text{CoFe}_2\text{O}_4/\text{N-SAC}$ which calcined at different temperatures, the XPS measurements were carried out. As shown Figure 2, the XPS spectra of Co 2p, Fe 2p, C 1s, N1s and O 1s were obtained with the characteristic absorption peaks appear at 284.62 eV, 399.59 eV, 532.53 eV, 711.27 eV and 780.87 eV, respectively, and the corresponding element contents in various samples are shown in Table 2. Compared with SAC, $\text{CoFe}_2\text{O}_4/\text{N-SAC}$ prepared at different calcination temperatures showed characteristic absorption peaks of N1s, indicating that nitrogen was successfully doped into sludge-based activated carbon. Moreover, the absorption peak of O1s decreased obviously, which indicated that some oxygen-containing groups reacted with the amino group of polyacrylamide in the process of nitrogen doping.

In order to further study the existing forms and changes of N in $\text{CoFe}_2\text{O}_4/\text{N-SAC}$ at different calcination

temperatures, the peaks of N1s in these materials was fitted. The specific results are as follows:

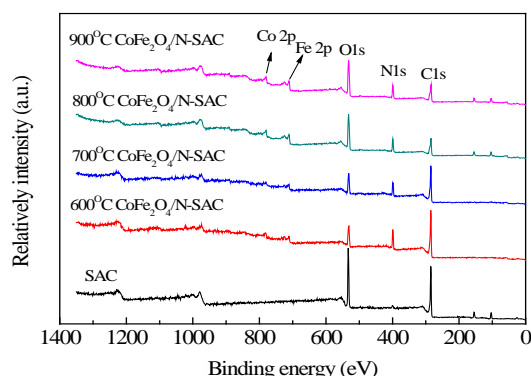


Figure 2. XPS spectra analysis of the different samples

Figure 3 shows the peak fitting spectra of N1s at different calcination temperatures from 400 °C to 800 °C. The peaks locate at 398.3 eV, 399.3 eV, 400.5 eV, 401.2 eV and 406.4 eV correspond to pyridine nitrogen, amino or imino ($-\text{NH}_2/-\text{NH}-$), pyrrole nitrogen, graphitized nitrogen and nitrogen oxides [17], respectively. In addition, the content of pyridine nitrogen increases with the increase of temperature when the calcination temperature is lower than 800 °C, but declines when the calcination temperature further increases to 900 °C, while the content of pyrrolic nitrogen and graphitized nitrogen increases with the increase of calcination temperature. This may be attributed to the transformation from pyridine nitrogen to pyrrolic nitrogen at higher temperature [18].

Table 1 Contents of elements in different samples

Sample	C(wt%)	O(wt%)	N(wt%)	Fe(wt%)	Co(wt%)	Co/Fe (mole ratio)
SAC	59.80	28.48	-	-	-	-
600°C $\text{CoFe}_2\text{O}_4/\text{N-SAC}$	58.15	16.78	15.86	12.46	4.07	1:3.23
700°C $\text{CoFe}_2\text{O}_4/\text{N-SAC}$	53.08	18.62	14.48	12.52	5.94	1:2.22
800°C $\text{CoFe}_2\text{O}_4/\text{N-SAC}$	31.70	24.30	13.49	13.49	7.17	1:1.98
900°C $\text{CoFe}_2\text{O}_4/\text{N-SAC}$	26.56	27.38	12.33	14.30	7.66	1:1.97

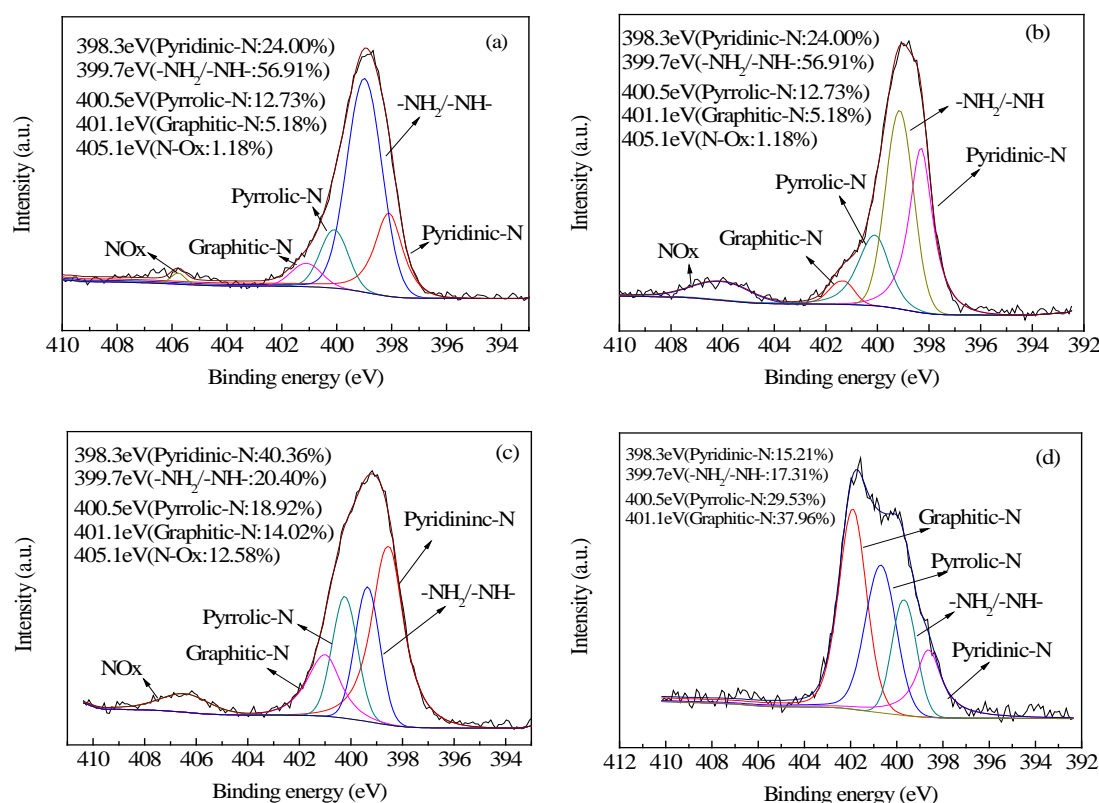


Figure 3. XPS spectrum of N1s at (a) 600°C, (b) 700°C, (c) 800°C and (d) 900°C

3.1.3 VSM

The magnetization curve of CoFe₂O₄/N-SAC is shown in Fig.4. That catalyst possessed a typical ferromagnetic hysteresis, with the Saturation magnetization (M_s) of 32.564 emu/g, residual magnetization (M_r) of 14.217 emu/g and coercive force of 134.11 G. Nonzero coercive force and residual magnetization proves the non superparamagnetic properties of the synthesized composite^[19]. The minimized coercivity ensures that the CoFe₂O₄/N-SAC does not become permanently magnetized after exposure to an external magnetic field, which in turn permits the composite particles to be re-dispersed without aggregation when the magnetic field is removed^[20]. The inset in Fig.4 affirms that the composite could be easily separated and reused from solution by applying an external magnetic field, which is beneficial to its practical application in wastewater treatment.

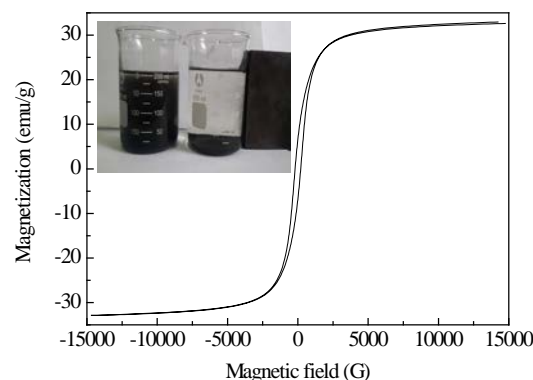


Figure 4. Magnetization curve of CoFe₂O₄/N-SAC

3.2 Influence of Calcination temperature on catalytic effect of catalyst

As shown in Fig.5, the effect of calcination temperature on the catalytic activity of CoFe₂O₄/N-SAC was studied. The results show that the effect of the calcination temperature on TOC removal is significant. The TOC removal rate of the coking wastewater increases from 50.34% to 80.53% with the increase of temperature from

500 to 800°C, but the removal rate of TOC decreases when the temperature is further increased to 900°C.

Cobalt ferrite has an ideal inverse spinel structure that contains different types of crystal faces in which the (111) plane exposes exclusively tetrahedral Fe^{3+} sites, the (100) face exposes the octahedral $\text{Co}^{2+}/\text{Fe}^{3+}$ sites. The chemical components exposed on the surface depended on the exposed crystal face of mixed oxides which dictated by the differences in surface energy between the two component oxides. It has been demonstrated that the surface energy of iron oxide to be lower than that of cobalt oxide, suggesting the Fe^{3+} terminated (111) surfaces would be advantaged and it therefore seems reasonable to indicate that the small CoFe_2O_4 particles expose more Fe^{3+} (111) surfaces, while the larger particles formed with increased calcination temperature expose more (100) facets thus increasing the Co/Fe ratio^[21]. The results of XPS in this study show that the ratio of Co/Fe (as shown in Tab.1) in the catalyst increases with the increase of calcination temperature, which is consistent with the results reported in the literature. Increasing surface Co^{2+} content is beneficial to catalysis. The removal rate of TOC increased with the increase of calcination temperature from 500 to 800 °C mainly ascribe to the larger CoFe_2O_4 nanoparticles at higher calcinated temperature have more Co rich surfaces and are more active towards organic pollutant decomposition than their smaller counterparts at lower calcinated temperature. When the calcination temperature further increased to 900°C, the ratio of Co/Fe does not increase remarkably but the removal rate of TOC decreased due to the agglomeration of CoFe_2O_4 .

Moreover, the influence of calcination temperature on the carrier is mainly manifested in the change of nitrogen structure. It can be seen from the XPS spectra of N1s (As shown in Fig.9) at different calcination temperatures that nitrogen with different chemical structures appears at different calcination temperatures. Previous studies have shown that nitrogen-doped carbon materials exhibit higher catalytic activity in catalytic reactions. But there is still a great deal of controversy about which type of nitrogen plays a major role in catalysis. Luo et al^[22] demonstrated that pyridine nitrogen, containing a pair of lone electron, could effectively convert the valence band structure of carbon materials and enhance the π state.

Long et al^[23] found that graphitized nitrogen was the active site of catalysis. Sun et al^[13] proved that graphitized N play a dominant role for PMS activation by theoretical calculation. Guo et al^[14] proved that pyridine nitrogen was the main active site in the oxygen reduction reaction of nitrogen-doped carbon materials by template catalyst.

In this experiment, the result shows that pyridine nitrogen was the highest at the calcination temperature of 800 °C, and the catalytic activity is best at that calcination temperature, which could be concluded that the pyridine-N is the main active site in this catalytic reaction and this conclusion is consistent with Guo's report.

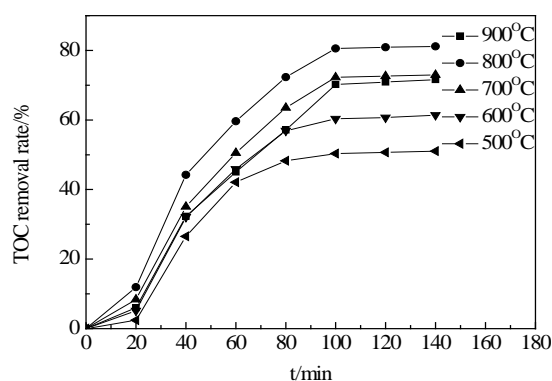


Fig.5 Effect of calcination temperature on TOC removal rate

4. Conclusions

A heterogeneous catalyst $\text{CoFe}_2\text{O}_4/\text{N-SAC}$ was synthesized and characterized. That catalyst is ferromagnetic with the Saturation magnetization (M_s) of 32.564 emu/g, residual magnetization (M_r) of 14.217 emu/g and coercive force of 134.11G, which could be easily separated and reused from solution by applying an external magnetic field. The effect of the calcination temperature on the catalytic performance of $\text{CoFe}_2\text{O}_4/\text{N-SAC}$ was investigated. The results indicated that the chemical components exposed on the surface and the chemical structures of N were influenced by the calcination temperature.

Acknowledgments

The authors gratefully acknowledge the financial support from the National Nature Science Foundation of Liaoning

Province of China (Grant No. 20170540452), and Major Science and Technology Platform Program of Engineering Research Center of Advanced Coal & Coking Technology and Efficient Utilization of Coal Resources, the Education Department of Liaoning Province (Grant No. USTLKFZD 2016340)

Reference

1. G.P. Anipsitakis, D.D. Dionysiou, *Environ. Sci. Technol.* **37**, 4790-4798 (2003).
2. H. Longxing, Y. Fan, Z. Lianpei, *Chin. Catal.* **36**, 1785–1797 (2015).
3. G.P. Anipsitakis, D.D. Dionysiou, *Environ. Sci. Technol.* **38**, 3705-3713 (2004).
4. G.P. Anipsitakis, E. Stathatos, D.D. Dionysiou, *Phys. Chem. B.* **109**, 13052-13055 (2005).
5. W. Bian, Z. Yang, P. Strasser, *Power Sour.* **250**, 196–203 (2014).
6. X. Yujiao, B. Weiyong, W. Jiao, *Electrochim. Acta.* **151**, 276–283 (2015).
7. H. Zhuang, H. Han, B. Hou, *Bioresour. Technol.* **166**, 178–186 (2014).
8. A. Abdedayem, M. Guiza, A. Ouederni, *C. R. Chim.* **18**, 100–109 (2015).
9. L. Hao, D. Huiping, S. Jun, *Mol. Catal.* **364**, 101–107 (2012).
10. P. Rai, R.K. Gautam, S. Banerjee, *Environ. Chem. Eng.* **3**, 2281–2291 (2015).
11. M. Wang, P. Zhang, J. Li, *Chin. Catal.* **35**, 335–341 (2014).
12. J. Wu, H. Gao, S. Yao, *Sep. Purif. Technol.* **147**, 179–185 (2015).
13. D. Xiaoguang, A. Zhimin, S. Hongqi, *ACS Appl. Mate. Interfaces.* **7**, 4169-4178 (2015).
14. G. Donghui, R. Shibuya, C. Akiba, *Science.* **351**, 361-365 (2016).
15. E. Kacan, *Environ. Manag.* **166**, 116–123 (2016).
16. F. Huang, C. Chen, F. Wang, *Catal. Surv. Asia.* **21**, 143–149 (2017).
17. Y. Xia, R. Mokaya, *Adv. Mater.* **16**, 1553-1558 (2004).
18. M. Zhigang, C. Xiaoye, D. Yukou, *Appl. Surf. Sci.* **2**, 1704–1710 (2011).
19. X. Lejin, W. Jianlong, *Environ. Sci. Technol.* **46**, 10145–10153 (2012).
20. J. Dong, Z. Xu, S.M. Kuznicki, *Adv. Funct. Mater.* **19**, 1268-1275 (2009).
21. Z. Luo, S. Lim, Z. Tian, *Mater. Chem.* **21**, 8038-8044 (2011).
22. J. Long, X. Xie, J. Xu, *ACS. Catal.* **2**, 622-631 (2012).
23. Y. Qiujing, C. Hyeok, R. Souhail, *Appl. Catal. B-Environ.* **88**, 462-469(2009).